Linear and nonlinear optical properties of SrBi4Ti4O15 thin films

A. Rambabu, E. Sivanagi Reddy, Syed Hamad, K. C. James Raju, and S. Venugopal Rao

Citation: AIP Conference Proceedings **1728**, 020339 (2016); doi: 10.1063/1.4946390
View online: http://dx.doi.org/10.1063/1.4946390
View Table of Contents: http://scitation.aip.org/content/aip/proceeding/aipcp/1728?ver=pdfcov
Published by the AIP Publishing

Linear and Nonlinear Optical Properties of $SrBi_4Ti_4O_{15}$ Thin Films

A. Rambabu[1], E. Sivanagi Reddy[2], Syed Hamad[1], K.C. James Raju,[1,2,a]
S. Venugopal Rao[2]

[1] School of Physics, University of Hyderabad,Hyderabad, Telangana 500046, India.
[2] Advanced Center of Research in High Energy Materials (ACRHEM), University of Hyderabad,Hyderabad, Telangana 500046, India.

[a] Author for correspondence: kcjrsp@uohyd.ernet.in

Abstract. Polycrystalline $SrBi_4Ti_4O_{15}$ thin films with good morphology and layered perovskite structure were fabricated on fused silica substrates using r f magnetron sputtering system at various oxygen mixing percentages (25 and 50). The crystallite sizes of the particles are in 17-28 nm range. The Nonlinear optical properties were investigated by using Z-scan method at a wavelength of 800 nm with 2 ps duration pulses. The films exhibit the fast and giant optical nonlinearities having the two-photon absorption coefficient (β) with magnitude of 10^{-8}-10^{-9} cm/W and the nonlinear refraction coefficient of ~10^{-12} cm^2/W. These results indicate $SrBi_4Ti_4O_{15}$ thin films are promising candidates for applications in nonlinear optical and optical signal processing devices.

INTRODUCTION

Ferroelectric oxides are characterized by switching of polarization, superior piezoelectric properties and high dielectric constant which leads to versatile applications like memories, sensors, energy harvesters and electro optical devices [1-2]. $SrBi_4Ti_4O_{15}$ (SBTi) is a lead free ferroelectric bismuth layered structure in Aurioullious family with general formula $(Bi_2O_3)^{2+}$ $(A_{m-1}B_mO3_{m+1})^{2-}$ where A site is mono-,di- or trivalent ions or mixture of them, B site is tetra, penta and hexa valent ions and m stands for number of perovskites inter leaved between (Bi_2O_3) layer. Our previous studies on r.f.sputtered SBTi thin films showed the effect of annealing temperature and oxygen mixing percentage of SBTi thin films [3-4]. SBTi thin films were mostly studied for high temperature sensor applications and memory devices.

EXPERIMENTAL

Thin films of SBTi were deposited on fused silica substrates by r.f.magnetron sputtering from lab-made SBTi targets. The SBTi ceramic targets were prepared in solid state reaction method and deposition of SBTi thin films was presented elsewhere [4]. In brief, the target was mounted on a magnetron cathode and power density was kept at $3W/cm^2$ with a fixed working pressure of 20mTorr by varying O_2 mixing percentage (25 and 50). The thin films were deposited at room temperature with thickness around 450 nm. The films were annealed both in conventional (C) and microwave (M) furnaces at 750^oC for 2 hours and 20 minutes respectively. For convenience, the samples were named as SBTiXY, where X (number) stands for Oxygen Mixing Percentage with Argon; Y (C or M) stands for type of annealing. The crystalline orientation and phase of the films were investigated by a Bruker D8 X-ray diffractometer with $CuK\alpha_1$ radiation of 1.5046 Å wavelength. The optical transmittance spectra of samples were recorded in the range 50-2500 nm using UV-Vis-NIR spectrophotometer (JASCO V-570) at room temperature. The

International Conference on Condensed Matter and Applied Physics (ICC 2015)
AIP Conf. Proc. 1728, 020339-1–020339-4; doi: 10.1063/1.4946390
Published by AIP Publishing. 978-0-7354-1375-7/$30.00

nonlinear optical (NLO) properties were performed using single beam Z-scan technique at a repetition rate of 1 kHz with pulse duration ~2 ps at 800 nm.The complete fitting procedures are discussed elsewhere [5-7]

RULTS AND DISCUSSIONS

Figure 1. shows the XRD pattern of single phase crystalline $SrBi_4Ti_4O_{15}$ thin films on fused silica substrate. The films were polycrystalline in nature and having (119) as strong peak which indicates the deposited films are in bismuth layered structure family. The value of inter-planar distance of the films deposited at 50%-OMP is close to the standard JCPDS value. The intensity of the diffraction peak and crystallite size is high for films deposited at 50% of OMP, which indicates improved crystalline quality. The crystallite size of the films is calculated using Scherer's equation. As OMP increase from 25% to 50%, crystallite size increases from 17.8 to 23.8 nm for microwave annealed films and 24 to 28nm for conventional annealed films. The variations in crystallite size are confirmed from the broadening of the XRD pattern.

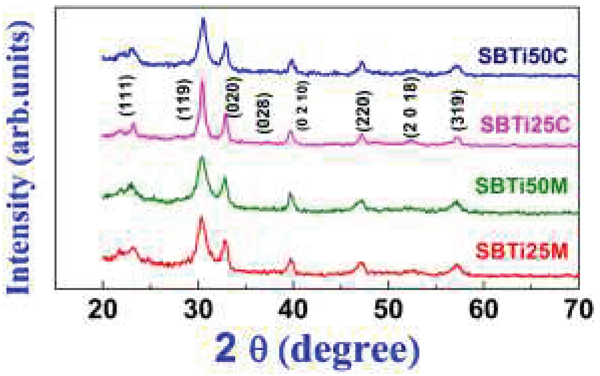

FIGURE 1. XRD pattern of SBTi thin films deposited on fused silica substrates.

The oscillations in transmission spectra of SBTi thin films [data shown in figure 2] arise due to the interference between SBTi film-substrate and SBTi film-air interfaces. The films are highly transparent in the visible region with transmittance of 60 to 80%. The band gap of the films is assumed as direct band gap and calculated from extrapolation of $(\alpha h\nu)^2$ versus $h\nu$ with $(\alpha h\nu)^2 = 0$. The band gap varied from 3.1 eV to 3.5 eV as deposition condition changes. The variation in the band gap is due to stress-induced distortion of the band by substrate and film interaction and depends on the film processing parameters. The defects in the film are due to oxygen pressure variation and crystallite size. The films with smaller crystallite sizes exhibited the larger band gap energy than those with larger crystallite sizes.

The microstructures (images are not shown) of these films are strongly depending on OMP. The films deposited at 50% OMP shows the larger grain size than the other films. The average grain sizes of the films deposited at 25-50% are ranging between 132-110nm. The average grain size of the films annealed in a conventional furnace exhibited uniform grain size than the microwave annealed films.

The NLO properties of SBTi thin films were measured with single beam Z scan method. Figure 3(a) depicts the open aperture (OA) data recorded for SBTi thin films at a peak intensity of ~80 GW/cm^2 (blue solid line, upper curve) and 150 GW/cm^2 (orange solid line, lower curve). The signatures in all the scans indicated simply reverse saturable absorption (RSA). RSA is characteristic for optical limiting phenomena which can be used in optical limiting sensors to protect from high intense lasers. In order to quantify the NLO coefficients, OA Z-scan data were fitted using the standard Z-scan equations and a good fit was obtained for two photon absorption coefficient (β) with magnitudes of 10^{-8} to 10^{-9} cm/W.

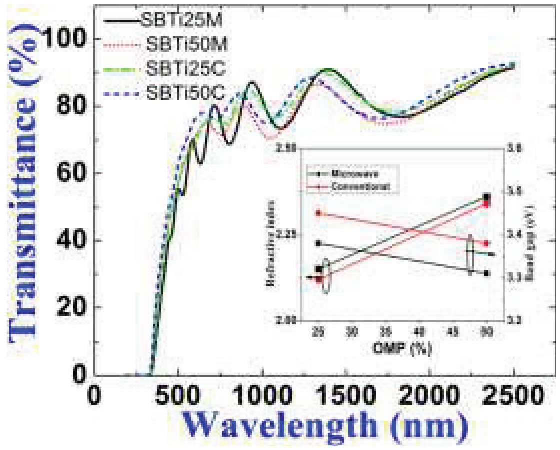

FIGURE 2. Transmission spectra of SBTi thin films (Inset) Variation of refactive index and the band bap with oxygen mixing percentage**.**

The values of β were slightly larger at higher peak intensities suggest that excited state absorption (1+1 photon absorption) could have contributed partially to the nonlinear absorption rather than pure two photon absorption (2PA). Even though the nonlinear absorption effects are combinedly from SBTi thin film and fused silica substrate, the contribution of nonlinear absorption from the amorphous fused silica substrate was negligible. This was confirmed by recording the Z-scan data of pure substrate and we did not observe any transmittance changes either in open aperture data or the closed aperture data.

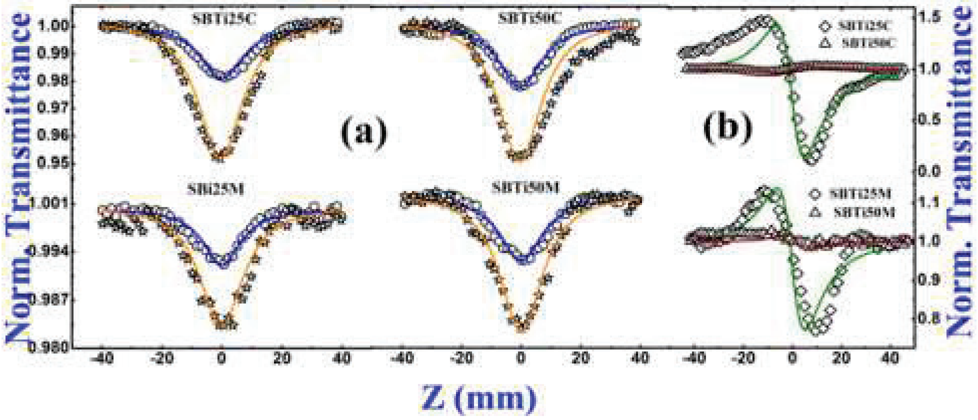

FIGURE3. (a) Open aperture Z-scan curves obtained for SBTi25C, SBTi50C, SBTi25M and SBTi50M with varying input peak intensities I_{00} = 80 GW/cm^2 (open circles) and I_{00} = 150 GW/cm^2 (open stars), respectively, and (b) Closed aperture Z-scan data obtained for SBTi25C, SBTi50C, SBTi25M and SBTi50M at a peak intensity of 55 GW/cm^2. Open stars, circles, diamonds represent experimental data while the solid (coloured) lines represent their respective theoretical fits.

Figure 3(b) illustrates the closed aperture (CA) Z-scan traces for all the films. The sign and magnitude of nonlinear refractive index (n2) were retrieved from CA Z-scan measured at a peak intensity of 55 GW/cm^2 and the data is presented in table 1. The peak and valley signature shows the self-defocusing property and is shown by negative refractive index n_2 except for SBTi50C. The self-defocusing situation is related to irradiation (laser duration and wave length) and intrinsic property of the SBTi thin films. SBTi50C demonstrated focusing property due to positive sign of refractive index n_2.

TABLE 1. Summary of NLO coefficient studies for all the SBT films and their physical properties.

Sample	2PA (β) 10^{-9} (cm/W)	n_2 10^{-12} (cm^2/W)	Crystallite Size (nm)	Surface roughness (nm)	Band gap (eV)
SBTi25C	17 (80 GW/cm^2) 25 (150 GW/cm^2)	-20.0	24.0	4.4	3.45
SBTi50C	13 (80 GW/cm^2) 18 (150 GW/cm^2)	0.9	28.0	4.9	3.42
SBTi25M	6.7 (80 GW/cm^2) 8.0 (150 GW/cm^2)	-5.0	17.8	4.4	3.35
SBTi50M	9.2 (80 GW/cm^2) 11 (150 GW/cm^2)	-0.6	23.8	9.2	3.31

CONCLUSIONS

In summary, $SrBi_4Ti_4O_{15}$ thin films with good morphology were successfully grown on fused silica substrates in r f magnetron sputtering system. Films were crystallized using conventional and microwave annealing. Films deposited at 50%- OMP exhibited the better crystalline and optical properties than 25%-OMP films. The band gap and linear refractive index are observed from optical transmission measurements. Its nonlinear optical properties are calculated from Z scan measurements at wavelength 800 nm with laser duration of 2 ps. The nonlinear properties show SBTi thin films can be used in optical devices. This investigation also shows that the oxygen partial pressure in deposition and annealing method had a significant role in influencing optical properties of the thin films.

ACKNOWLEDGMENTS

ESNR acknowledges financial support from DRDO through ACRHEM. Authors acknowledge the facilities provided by School of Physics and Centre for Nanotechnology, UoH.

REFERENCES

1. I. Grinberg, D.V. West, M. Torres, G. Gou et al., Nature 503, 509–512 (2013)
2. M. Dawber, K. M. Rabe, and J. F. Scott Rev. Mod. Phys. 77, 1083 (2005)
3. A. Rambabu, E. Sivanagi Reddy and K. C. James Raju, AIP Conf. Proc. 1591, 878 (2014)
4. A. Rambabu , S. Bashaiah , K. C. James Raju, J Mater Sci: Mater Electron. 25,1172–1179 (2014).
5. M. Sheik-Bahae, A.A. Said And E.W. Vanstryland, Opt. Lett. 14, 955-957 (1989).
6. K. Venkata Saravanan, K.C. James Raju, M. Ghanashyam Krishna, Surya P. Tewari, S. Venugopal Rao, Appl. Phys. Lett. 96, 232905 (2010).
7. S. Hamad, S.P. Tewari, L. Giribabu, S. Venugopal Rao, J. Porphy. Phth. 16, 140-148 (2012).